Supplementary information

Outline

1. **Description of background for HDAC family members and HDACi specificity**
2. **Supplemental Table**
3. **Supplemental Figures 1-17**
4. **References**

1. **Background for HDAC family members and HDACi specificity**

HDACs interact with other chromatin-modifying enzymes and co-regulators and play a key role in shaping epigenetic landscapes[1]. There are a total of 18 HDAC enzymes in the mammalian genome and are generally divided into four classes including class I, II, III and IV, based on sequence homology to their yeast counterparts[2]. Among the HDACs, Class I, II and IV HDACs are the zinc-dependent hydrolases. Class I HDACs include 1, 2, 3, and 8, which have been well documented to exert deacetylase activity on histone substrates as well as non-histone substrates. These family members are all inhibited by the non-selective HDAC inhibitor sodium butyrate [3]. Class II HDACs can be divided into Class IIa members, which include HDAC 4, 5, 7 and 9, and Class IIb members, which include HDAC6 and 10. In the case of HDAC5, a role in the brain has been identified in response to both antidepressant action [4] and to chronic emotional stimuli [5]. However, whether class IIa HDACs themselves have functional histone (or other non-histone) deacetylates activity, rather than activity contributed by co-purifying class I HDACs, currently remains unclear [6]. Class IIb family members, HDAC6 and 10 are mainly localized in the cytoplasm. HDAC6 is unique in the family in its possession of two deacetylase domains. HDAC6 has been shown to function as both an α-tublin (K40) deacetylase and to regulate ubiquitin-dependent protein degradation by the proteasome [7]. In contrast, class III HDACs (sirtuins; SIRT1-7) are non-classical, NAD(+)-dependent enzymes, which exhibit a non-overlapping sensitivity to most structural classes of inhibitors of zinc-dependent HDACs, including SB. The latter finding suggests the sirtuins are not the relevant targets of HDACi induced memory enhancement.

2. Supplemental Table 1.

List of neuronal activity regulated genes and genes involved in synaptic plasticity, synaptogenesis and memory formation.

Gene name	Synaptic remodeling	Expression regulated by neuronal activity	Memory formation	Ref.
BDNF	+	+	+	8 9
PKM zeta	+		+	10
EGR1	+	+	+	11 12
CREB	+	+	+	13 14 15 16
CBP	+		+	17
Nrxn1, Nrxn3	+			18
CaMKII*alpha*	+		+	19
CDK5	+		+	20
EGR2		+		21
PSD95	+		+	22
Agrin	+			23
Homer1	+	+	+	24,25
Arc	+	+		24,26
c-fos	+	+	+	27 28
AMPA1	+		+	29
synaptophysin	+			30
Synapsin2	+			31
Shank3	+		+	32
P35	+		+	33
Cpg15	+	+		34 35
NR2B	+		+	36,37
NR2A	+		+	36,38
GluR2	+		+	39
SNK	+	+		40

3. Supplemental Figure

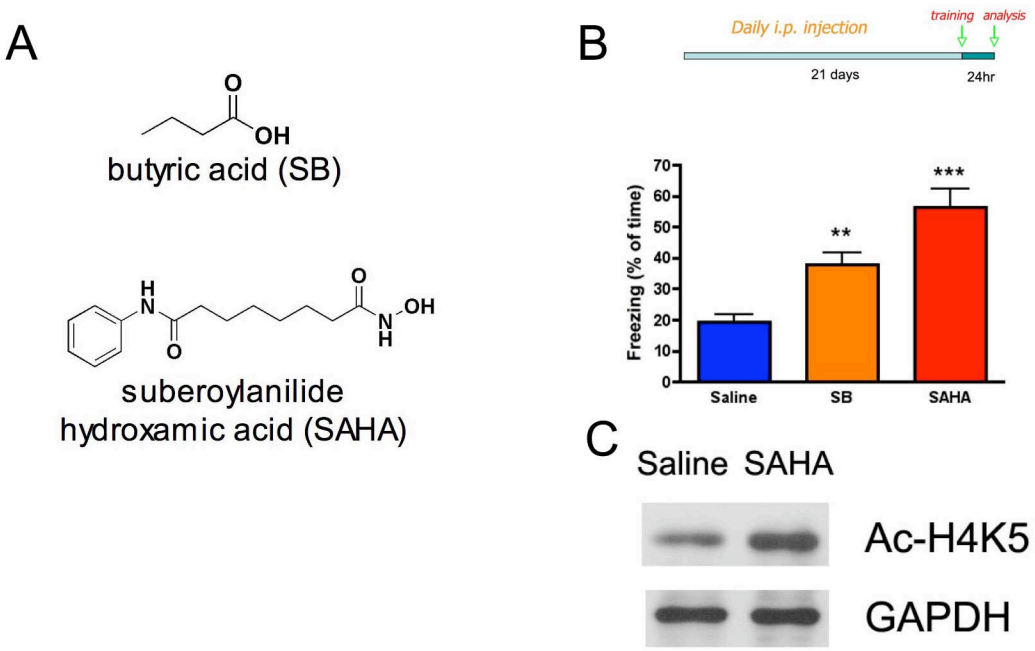

Supplemental Figure 1. Chronic treatment with HDAC inhibitors increased associative learning in mice.
(A) Structure of suberoylanilide hydroxamic (SAHA) and sodium butyrate (SB). (B) WT mice were injected with sodium butyrate (SB, 1.2g/kg, i.p., n=10), suberoylanilide hydroxamic acid (SAHA, 50mg/kg,i.p., n=8) or saline (n=8) for 21 days. Mice were subsequently subjected to contextual fear conditioning test 24 hours after training (**,$p<0.005$; ***, $p<0.0005$). (C) Western blot analysis of histone preparations revealed increased acetylation of H4K5 in the brain after chronic SAHA treatment (50mg/kg, i.p., for 21 days).

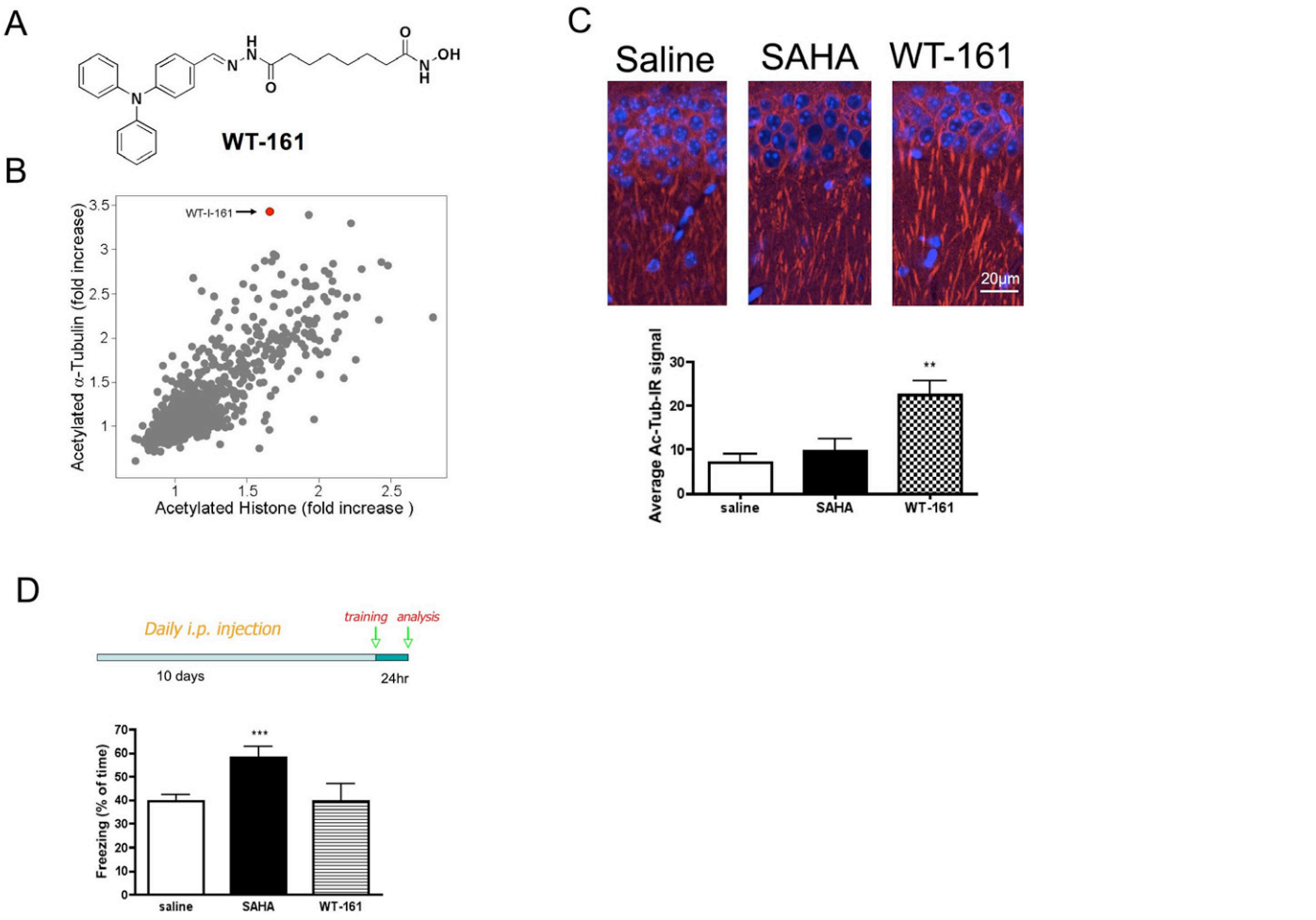

Supplemental Figure 2. Increased α-Tubulin(K40) acetylation resulting from HDAC6 inhibition does not facilitate associative learning in mice.

(A) Structure of WT-161. (B) Selectivity of WT-161 (2 μM) for increasing acetylated α-tubulin(K40) over total acetylated lysine (Ac-lysine) measured in human MM1.S cells treated for 16 hrs and assessed for hyperacetylated histones and/or α-tubulin(K40) using quantitative immunofluorescence imaging. Data presented are derived from a primary screen of a library of compounds biased for deacetylase function (J.E.B, manuscript in preparation). (C) Immunostaining of acetylated α-tubulin(K40) in area CA1 of hippocampus from mice treated with WT-161 or SAHA (both conditions in 25mg/kg, i.p., 10 days) or saline. Acetylated a-tubulin(K40) immunoreactive intensity signals in area CA1 were quantified (n=9, for each group). **, $p<0.005$. (D) Memory test of WT mice injected with SAHA (25mg/kg) or WT-161 (25mg/kg) for 10 days. Mice were subjected to contextual fear conditioning training 24 hours before test (WT, n=20; SAHA, n=20; WT-161, n=10; ***, $p<0.0005$, student *t*-test).

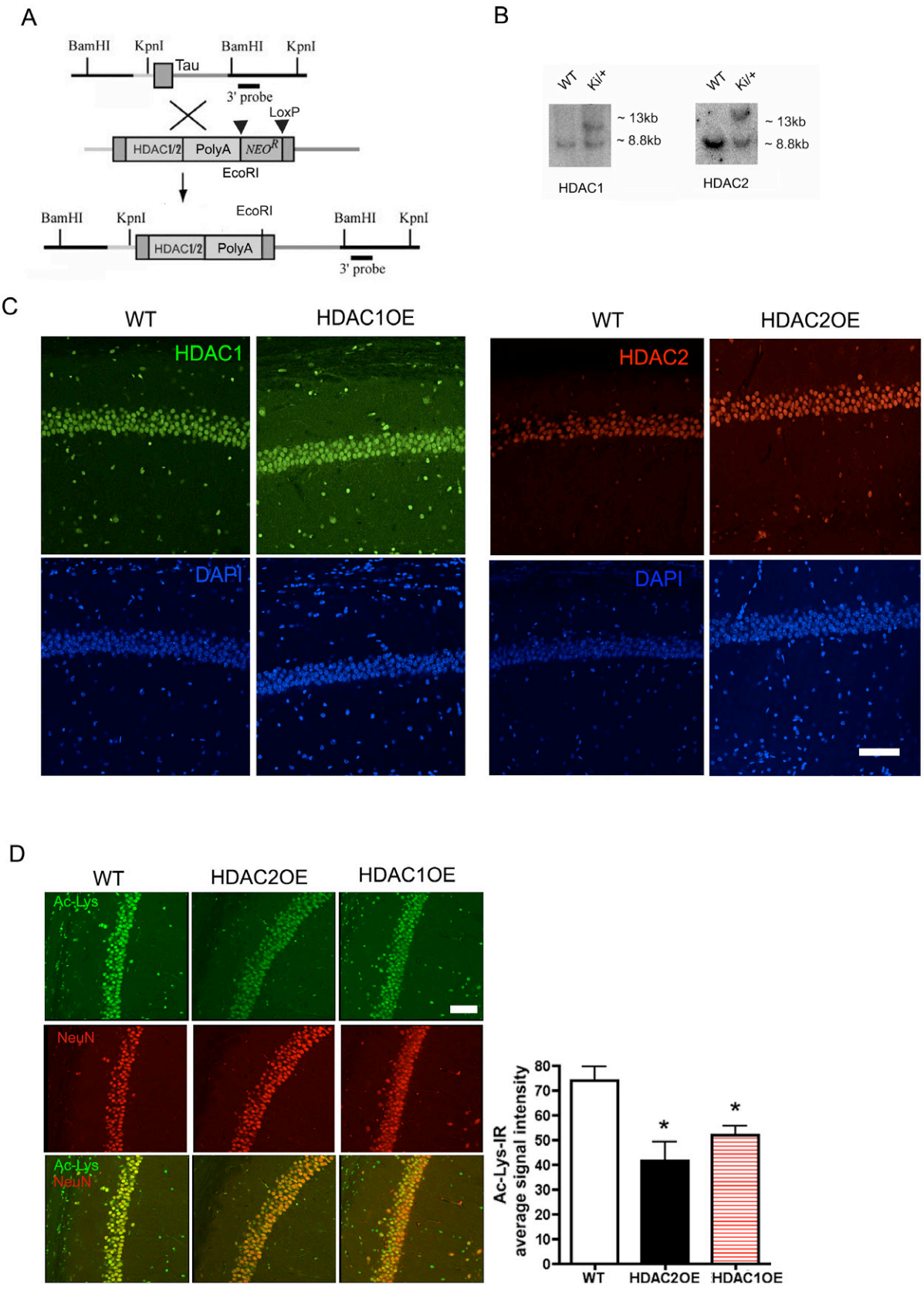

Supplemental Figure 3. Characterization of HDAC1OE mice and HDAC2OE mice

(A) Targeting strategy to insert the *HDAC1 or HDAC2* cDNA. (B) Southern blot analysis of targeted mice (ki/+). (C) Representative immunostaining images showing the expression of HDAC2 and HDAC1 in area CA1 of hippocampus from WT, HDAC2OE(ki/ki) and HDAC1OE(ki/ki) group. Scale bar, 100 μm. (D) Acetylation levels in hippocampal CA1 neurons. Immunostaining images for NeuN and Ac-lysine shows significantly decreased acetylation in the nucleus of pyramidal neuron of HDAC1OE mice (n=15, p=0.0298) and HDAC2OE mice (n=9, p=0.0128), when compared to WT mice (n=12). Optical intensity of Ac-lysine-immunoreactive signal was quantified in the pyramidal layer. Scale bar, 80 μm. *, $p<0.05$; *student t*-test, error bars are SEMs.

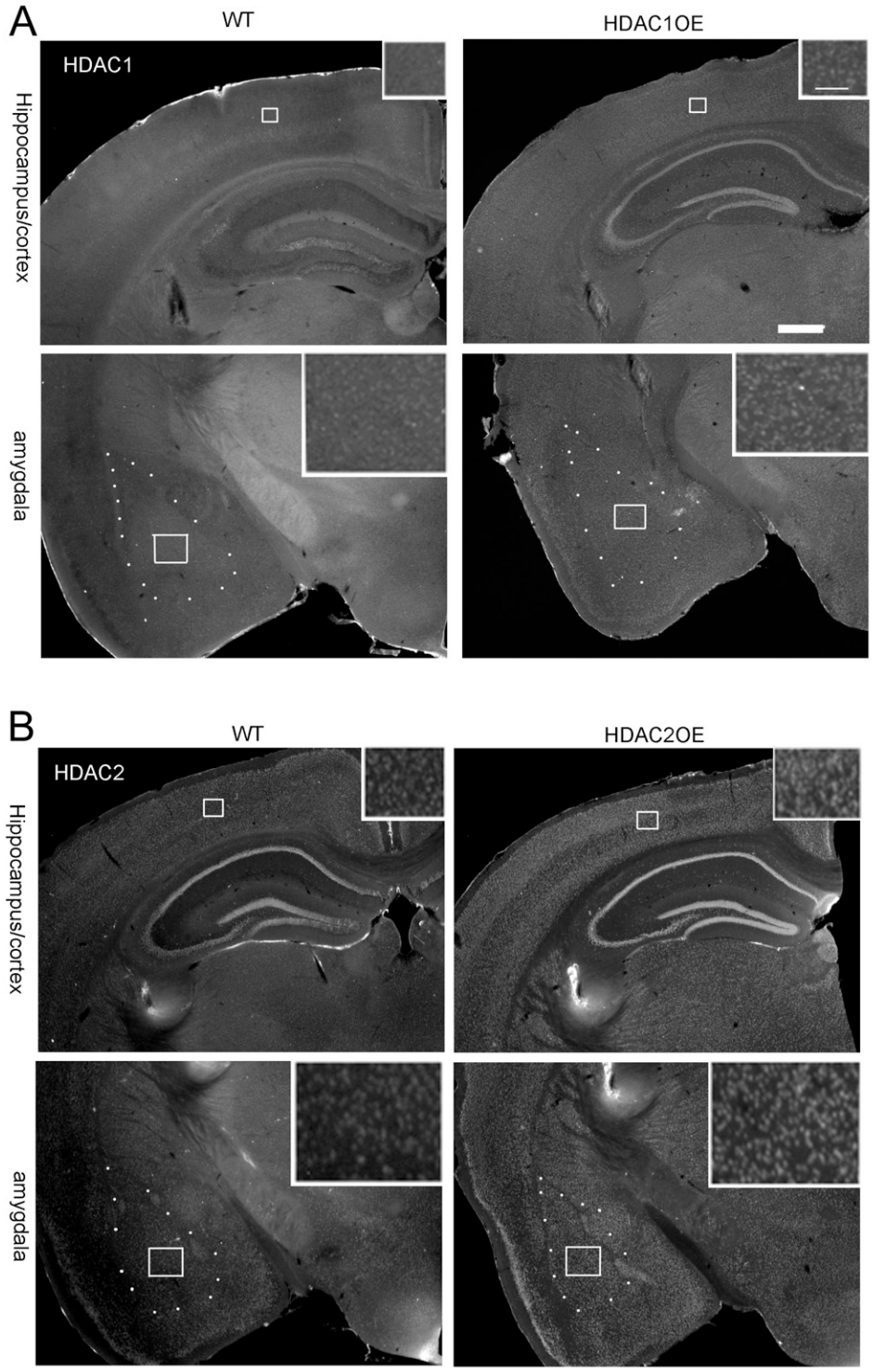

Supplemental Figure 4. Expression and distribution of HDAC1 and HDAC2 in HDAC1OE and HDAC2OE mouse brains.
(A) Representative immunostaining images showing the expression of HDAC1 in the WT and HDAC1OE mice brain. Note that in WT brain, HDAC1 expression level is relatively higher in dentate gyrus than other areas of the brain. Increased HDAC1 signal in HDAC1OE brain is detected not only in the hippocampus but also in the cortex, amygdala (indicated with dashed lines) and basal forebrain. (B) Representative immunostaining images showing the expression of HDAC2 in WT and HDAC2OE mouse brains. Scale bar, 400 μm. Scale bar for insertion, 100 μm

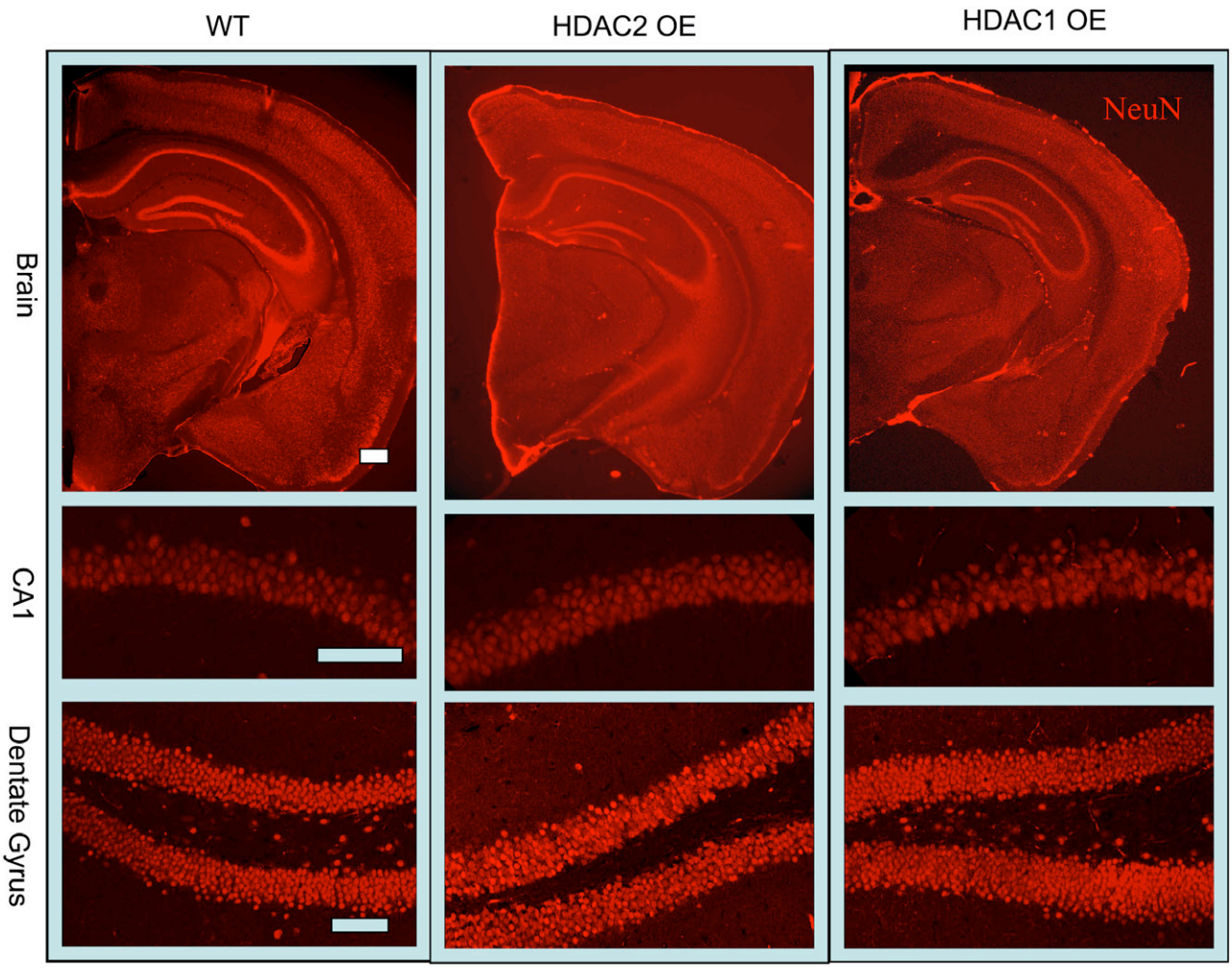

Supplemental Figure 5. Brain morphology of HDAC1OE and HDAC2OE mice
NeuN staining showed no obvious changes in brain architecture or neuron numbers in 6-month-old HDAC1OE and HDAC2OE mice. Scale bars, 100μm.

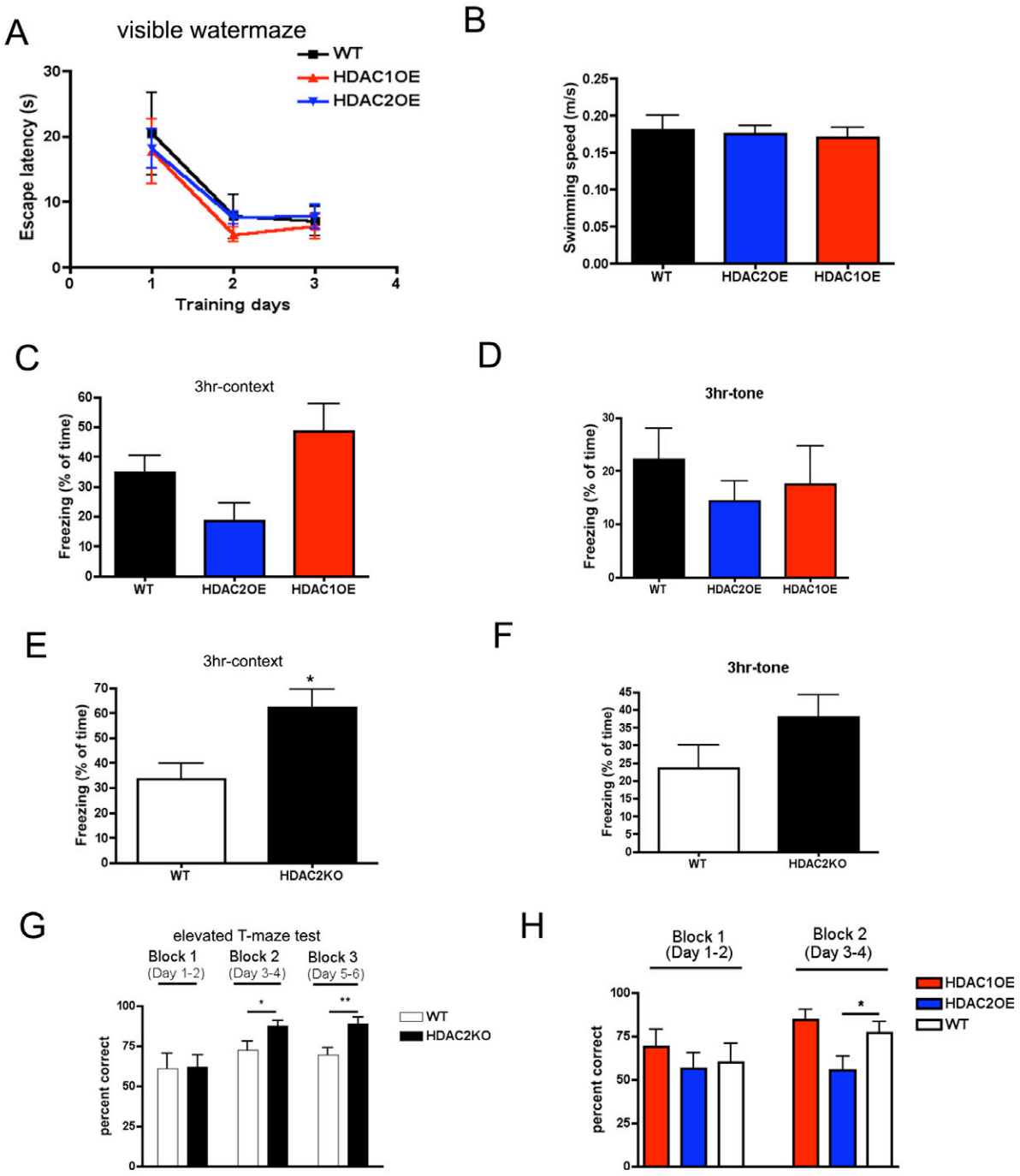

Supplemental Figure 6. HDAC2KO mice exhibit enhanced memory in behavior tasks.
(A) Escape latency of WT, HDAC1OE and HDAC2OE mice in the visible platform water maze test. Mice were trained in the swimming pool with a visible platform for 3 days, with two trials per training day. The latency for mice to reach the platform was quantified (n=8 for each group). All three groups of mice reached the platform with similar escape latencies on the first day. No significant difference in escape latency was detected between the three groups of mice during the 3 days of training. (B) Swimming speed in the water maze pool (n=8 for each group). (C-D) Short-term memory test for WT, HDAC1OE and HDAC2OE mice in contextual- and tone-dependent fear conditioning paradigms (WT, n=9; HDAC2OE, n=9; HDAC1OE, n=8). No significant difference was detected between the WT group and the HDAC1/2OE mice. (E-F) Short-term memory test for HDAC2KO mice in contextual- and tone-dependent fear conditioning paradigms (WT, n=8; HDAC2KO, n=9). HDAC2KO mice showed significantly increased freezing in contextual fear conditioning (p=0.0100, compared to WT littermates), but not in tone-dependent fear conditioning (p= 0.1439). (G) Mean percent correct responses for WT (n=8) and HDAC2KO mice (n=10) during spatial non-matching to place testing on the elevated T-maze. HDAC2KO mice showed significant higher accuracy during the training period (Block 2, p=0.044, Block 3, p=0.0087, student t-test; between genotypes, p=0.0252, two-way ANOVA). (H) Mean percent correct responses for WT (n=8), HDAC1OE (n=7) and HDAC2OE (n=9) mice during spatial non-matching to place testing on the elevated T-maze. HDAC2OE mice showed significant defects in accuracy during training trail block 2 (p= 0.0452, student t-test).

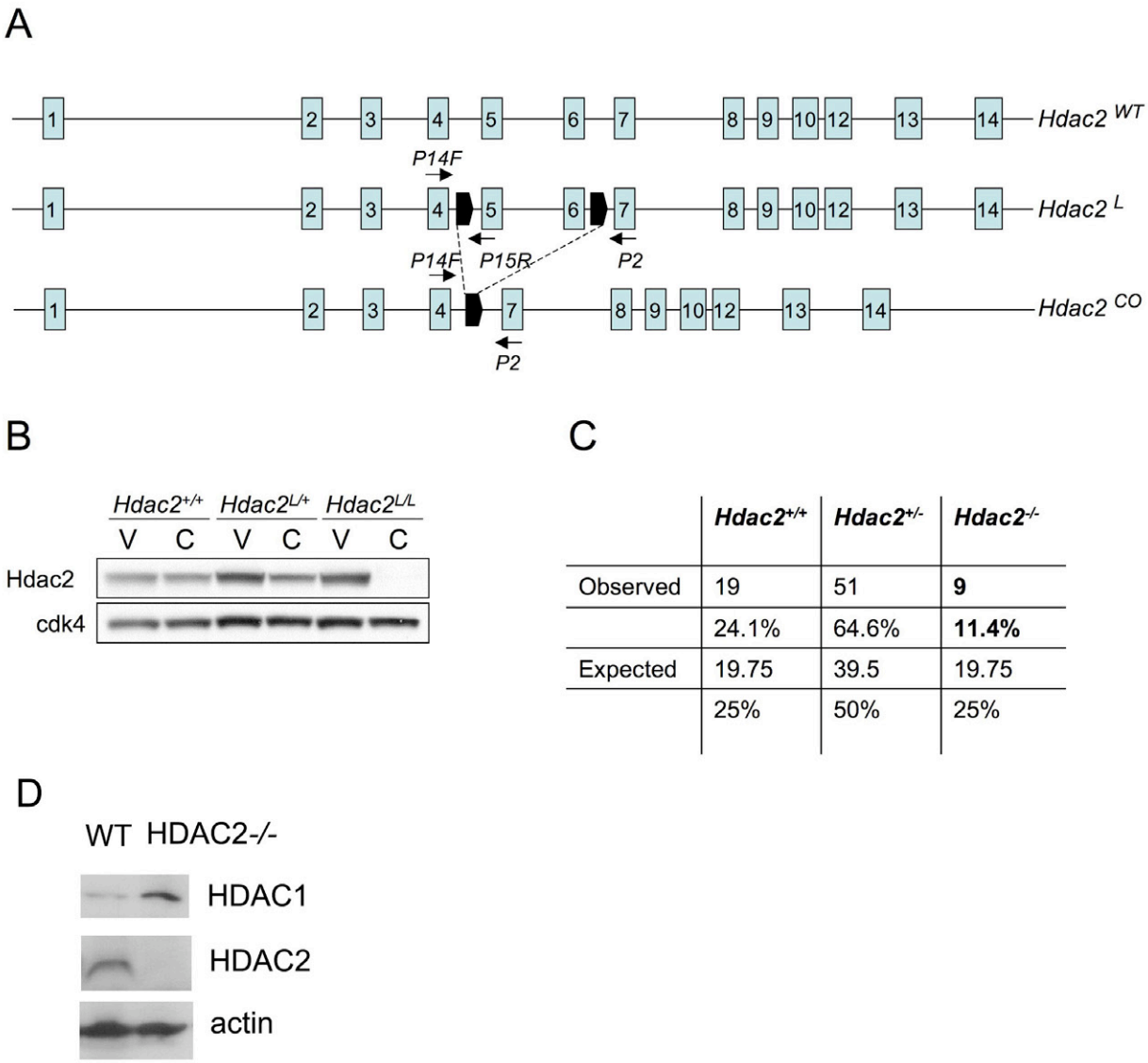

Supplemental Figure 7. Characterization of HDAC2KO mice.
(A) Schematic representation of the murine *Hdac2* genomic locus. Gray filled boxes indicate exons. Black arrowheads indicate *lox*P positions. P14F, P15R and P2 are oligo DNA primers used for genotyping. (B) Westernblot analysis of protein lysates obtained from wild-type, $Hdac2^{L/+}$ and $Hdac2^{L/L}$ MEFs infected with either vector (V) or Cre-recombinase expressing retroviruses, using HDAC2 specific antibodies. Cdk4 served as a loading control. (C) Observed and expected numbers and frequencies of wild-type, $Hdac2^{+/-}$ and $Hdac2^{-/-}$ mice obtained from multiple $Hdac2^{+/-}$ intercrosses. (D) Western blot analysis of HDAC1 and HDAC2 expression levels in the brain lysate from the $Hdac2^{-/-}$ mouse and WT littermate. Note that HDAC1 expression level was increased in $Hdac2^{-/-}$ mice.

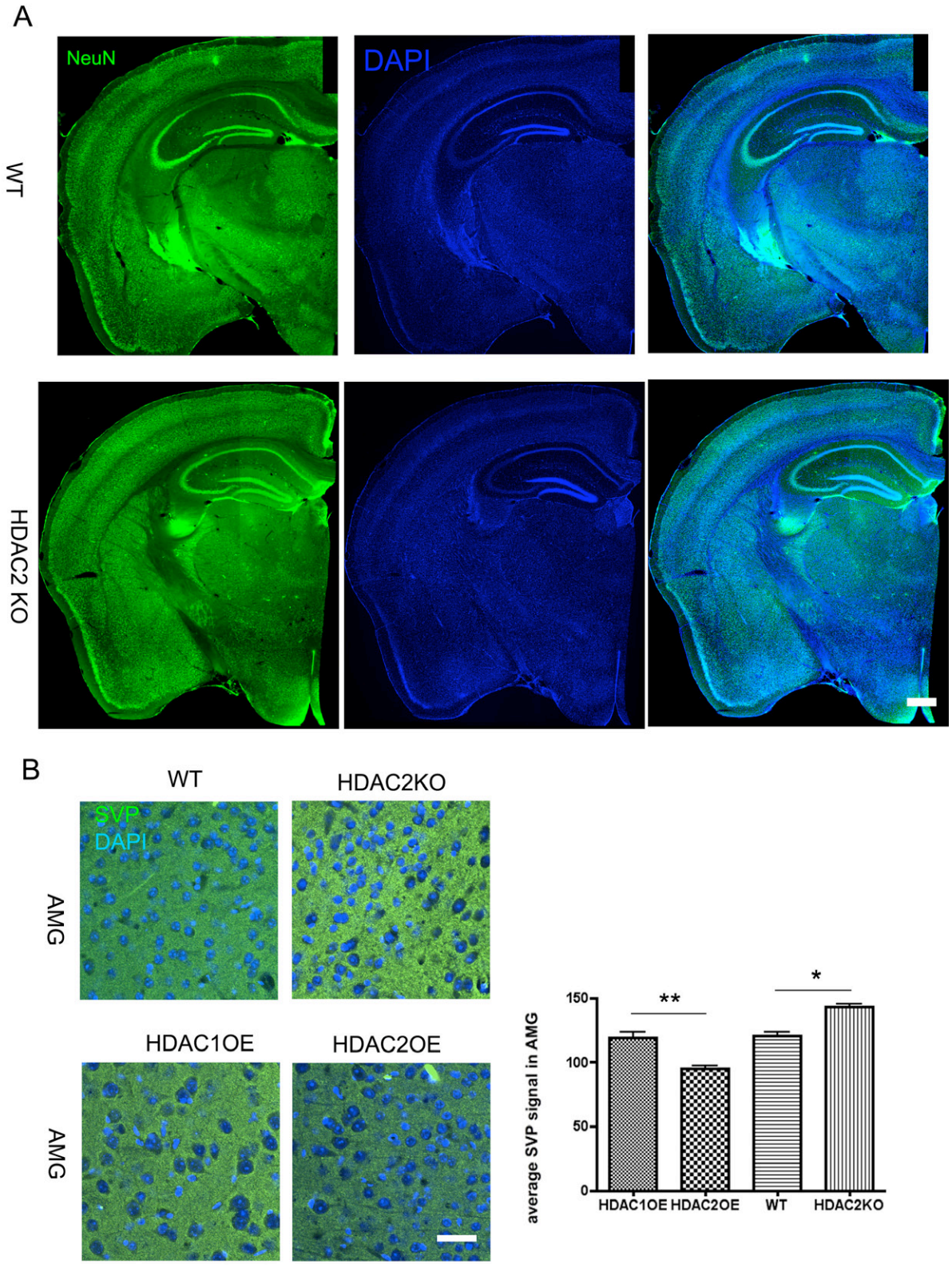

Supplemental Figure 8. Brain morphology of HDAC2KO mice

(A) NeuN and DAPI staining showed no obvious changes in brain architecture of 6-month-old HDAC2KO mice. Scale bar, 200μm (B) Synaptophysin staining in the amygdala (AMG) showed increased synapse numbers in HDAC2KO mice and decreased numbers in HDAC2OE mice (WT, n=5; HDAC2KO, n=6; HDAC1OE, n=5; HDAC2OE, n=5; *, $p<0.05$; **, $p<0.005$; student t-test). Scale bar, 80 μm.

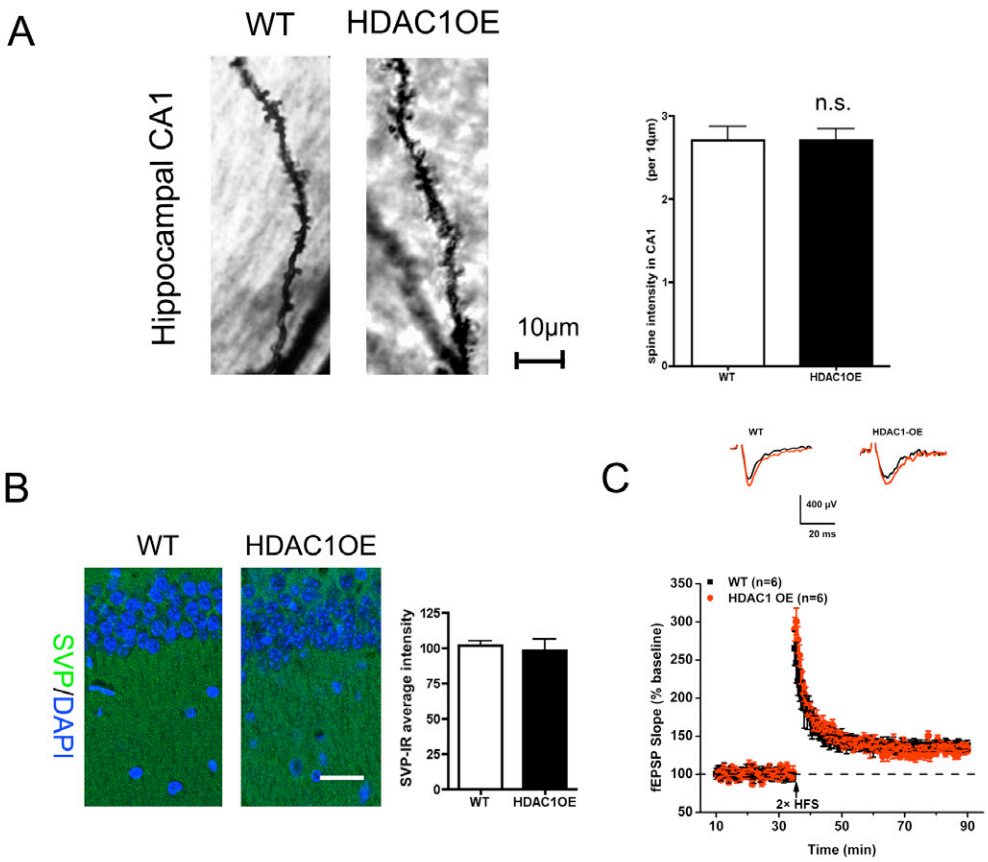

Supplemental Figure 9. HDAC1OE mice are similar with WT in synapse number and synaptic plasticity.
(A) Golgi impregnation showed no obvious differences in dendritic spine density in hippocampal area CA1 of HDAC1OE mice compared to WT (WT, n=19 dendrites; HDAC1OE, n=23 dendrites, p= 0.9835). (B) Synaptophysin staining in hippocampal CA1 area showed similar synapse number in HDAC1OE mice and WT (WT, n=6; HDAC1OE, n=8). Scale bar, 80 μm. (C) Long-term potentiation (LTP) was induced by two trains of HFS stimulation (2 x 100Hz, 1s) in area CA1 of the hippocampal slices prepared from 6 month old HDAC1OE mice or WT littermates. Forty min after the stimulation, the fEPSPs from HDAC1OE mice remained potentiated (132.8± 5.8 % compared with baseline), similar to the fEPSPs from the hippocampal slices prepared from control mice (135.8± 5.5 % compared with baseline).

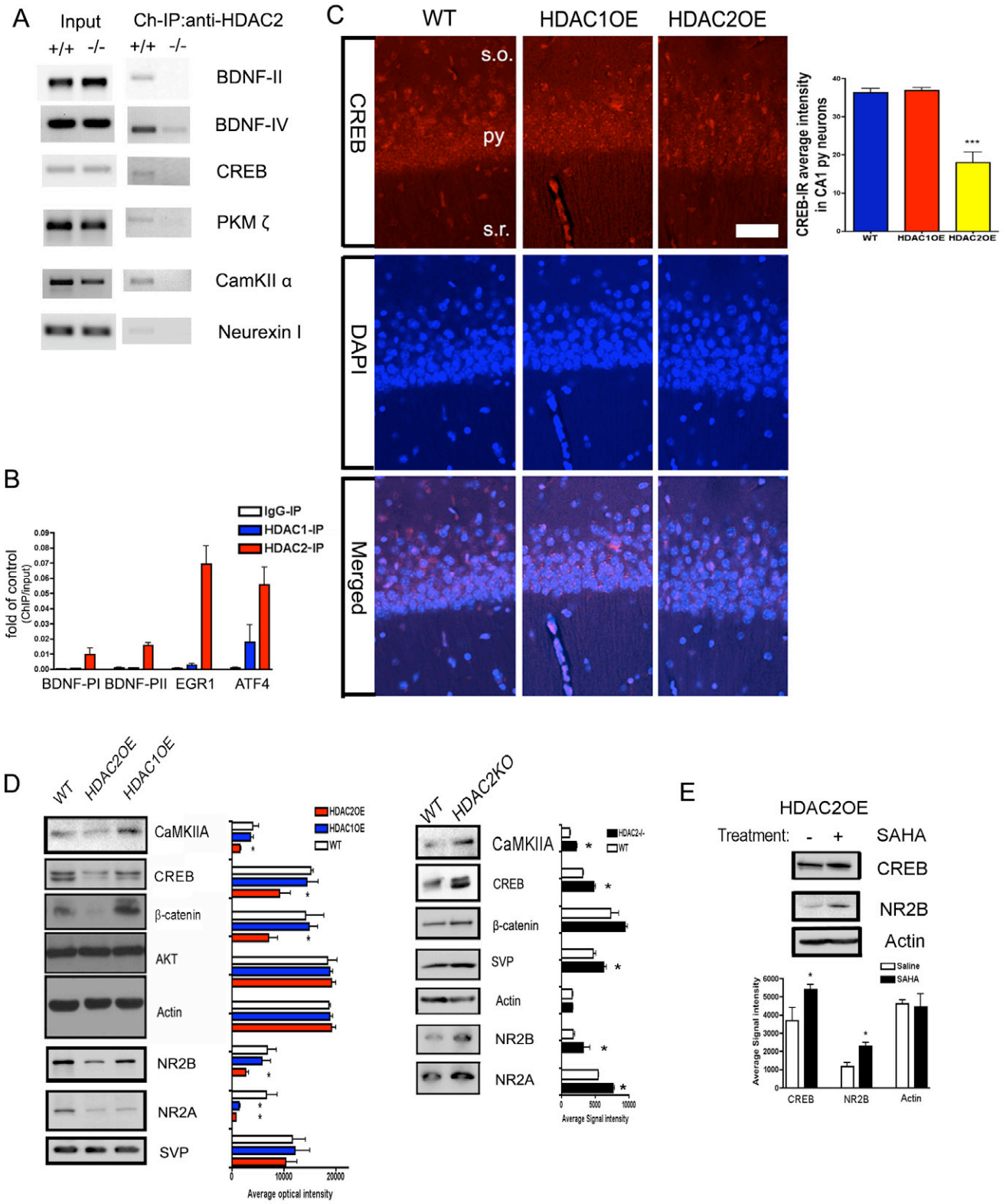

Supplemental Figure 10. HDAC2 is preferentially enriched in the promoter of genes associated with memory formation.

(A) Chromatin immunoprecipitation (ChIP) with anti-HDAC2 antibody showed strong signals with memory associated genes in WT but not in HDAC2 KO mouse samples. (B) Chromatin immunoprecipitated samples were extracted from mouse hippocampi and subjected to real-time, quantitative PCR (qPCR). (C) CREB expression in area CA1 of the HDAC overexpression mice. CREB-like immuno-reactive signal in the pyramidal layer was quantified. HDAC2OE mice showed less CREB expression in the pyramidal neurons compared to WT mice. No significant difference was detected between HDAC1OE and WT mice (WT mice, n=8; HDAC2OE mice, n=8; HDAC1OE mice, n=14, ***p<0.0005). Scale bar, 80μm (D) Western blot analysis of protein expression in the hippocampi of HDAC1OE, HDAC2OE and HDAC2KO mice. Signals from 3 independent experiments were quantified (*, $p<0.05$; *student t*-test, error bars are SEMs). (E) Western blot analysis of protein expression in HDAC2OE mice. SAHA (25mg/kg, i.p., n=3) was injected for 10 days.

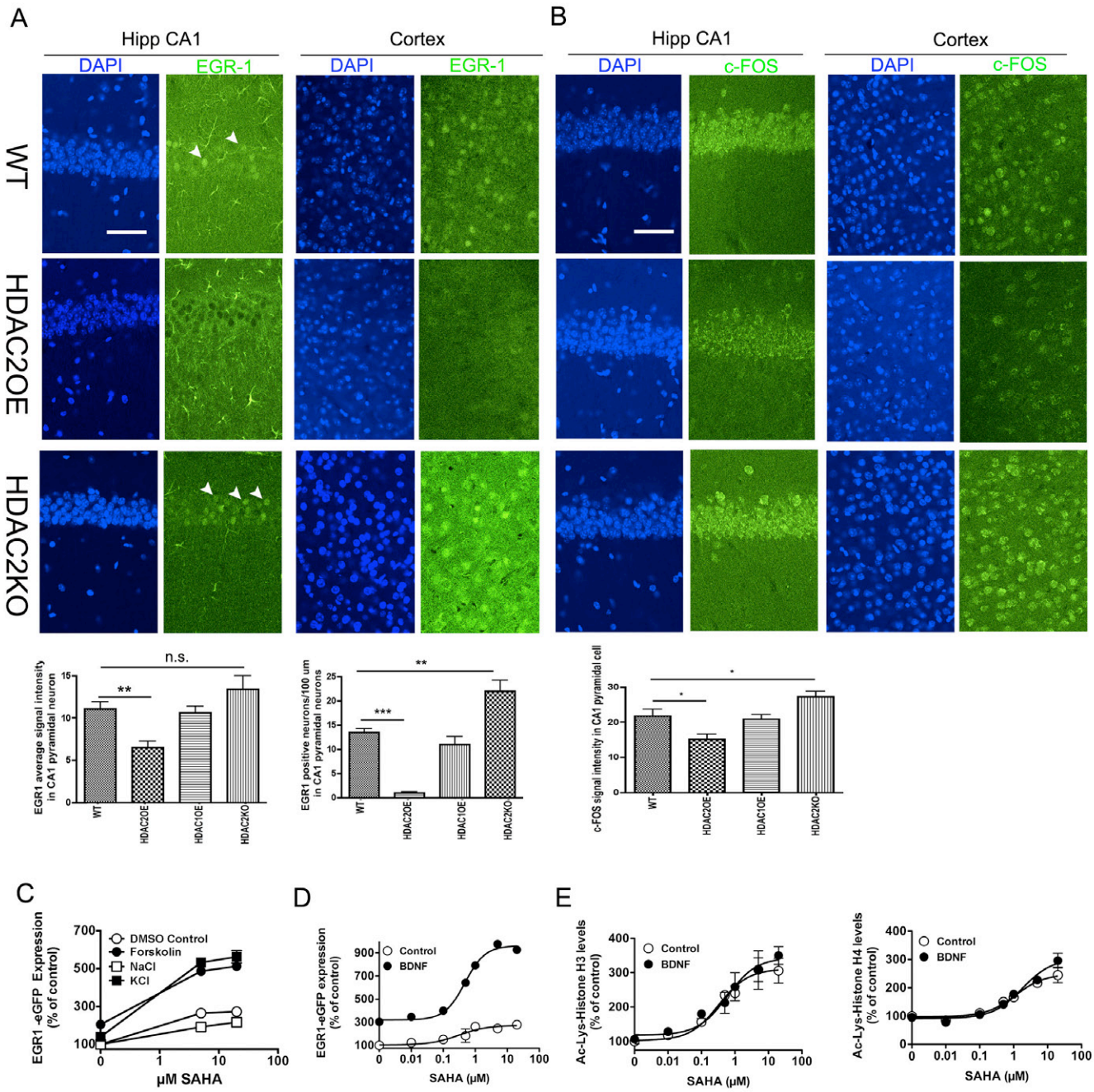

Supplemental Figure 11. HDAC2 regulates CREB target gene expression in mouse brain and in dissociated neurons.
(A-B) Expression of c-FOS and EGR1 are reduced in HDAC2OE mice and increased in HDAC2KO mice in area CA1 and cortical areas. Arrowheads indicate the EGR1-expressing neurons (*, $p<0.05$; **, $p<0.005$; ***, $p<0.0005$, *student t*-test, error bars are SEMs). Scale bar, 100 μm. (C-D) Quantitative assay for SAHA effects in dissociated cortical neurons from EGR1-GFP mice. All data were normalized to control group, which was treated with culture medium. (C) Inhibition of HDAC activity by SAHA pre-treatment potentiated KCl- (55mM) or forskolin- (50μM) induced EGR-1 expression in dissociated cortical neurons (treated with 40μM NBQX and 100μM AP5). (D) Dose-response curve of SAHA pre-treatment effect on EGR-1 expression with or without BDNF (50ng/ml) induction in dissociated cortical neruons. (E) Dose-response curve of SAHA pre-treatment effect on BDNF- (50ng/ml) induced Ac-lysine-histone 3/ 4 levels. SAHA pretreatment increased both Ac-H3 and Ac-H4 levels, which is comparable to its effect on potentiation of BDNF-induced EGR-1 expression. 3,000-5,000 cells were measured for each point on the assay. Error bars represent SEMs.

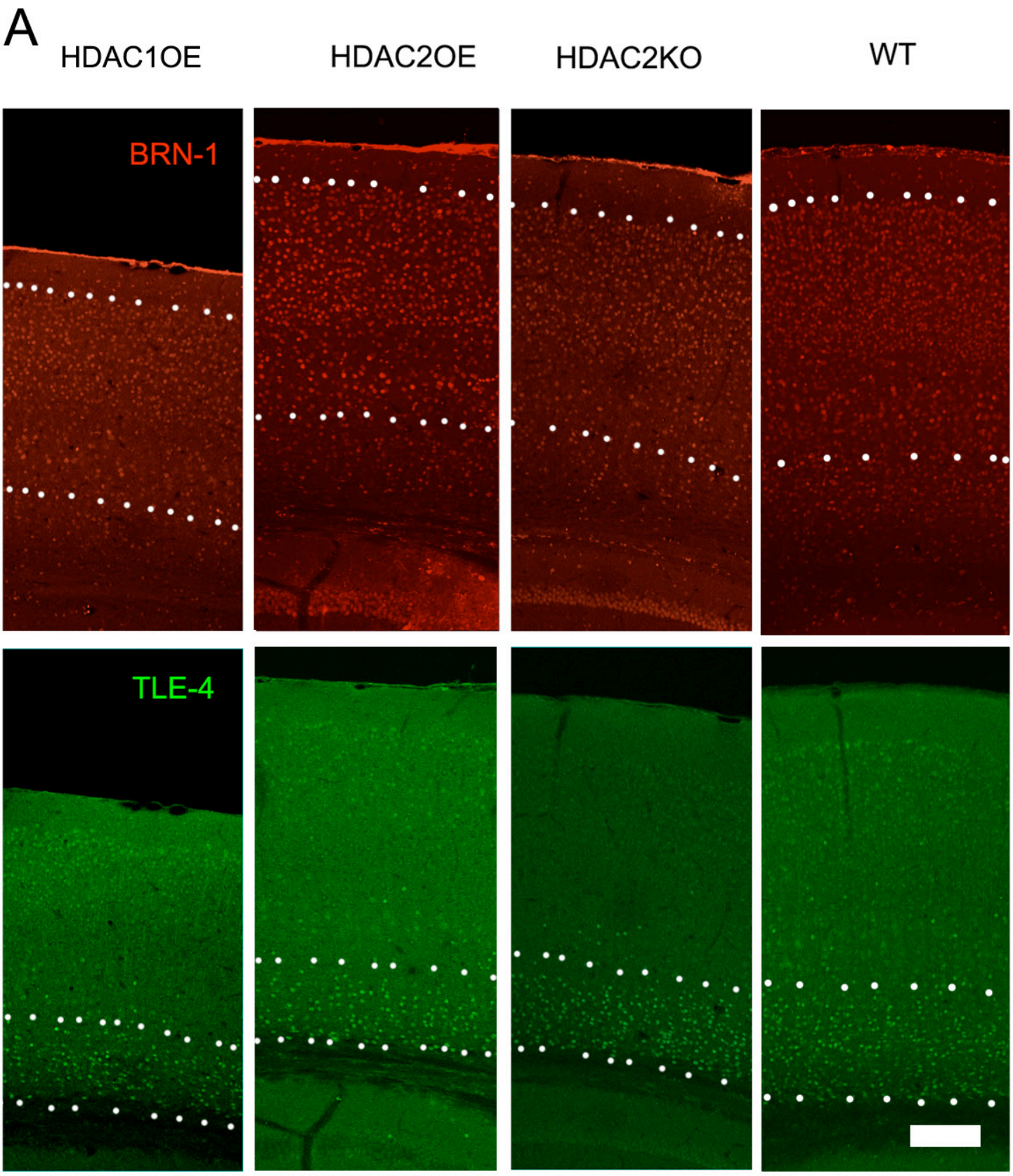
A
HDAC1OE
HDAC2OE
HDAC2KO
WT
BRN-1
TLE-4

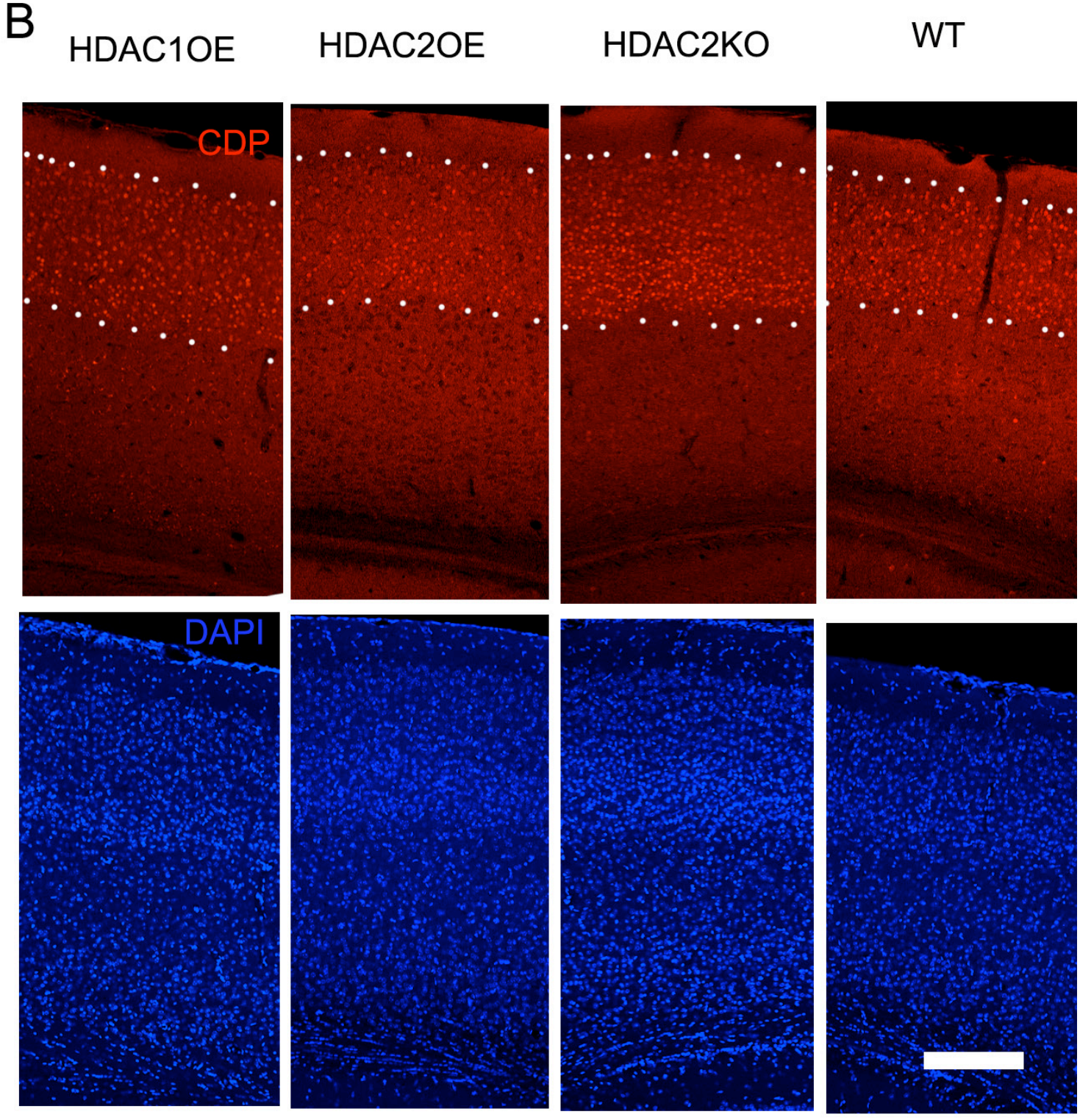
B
HDAC1OE
HDAC2OE
HDAC2KO
WT
CDP
DAPI

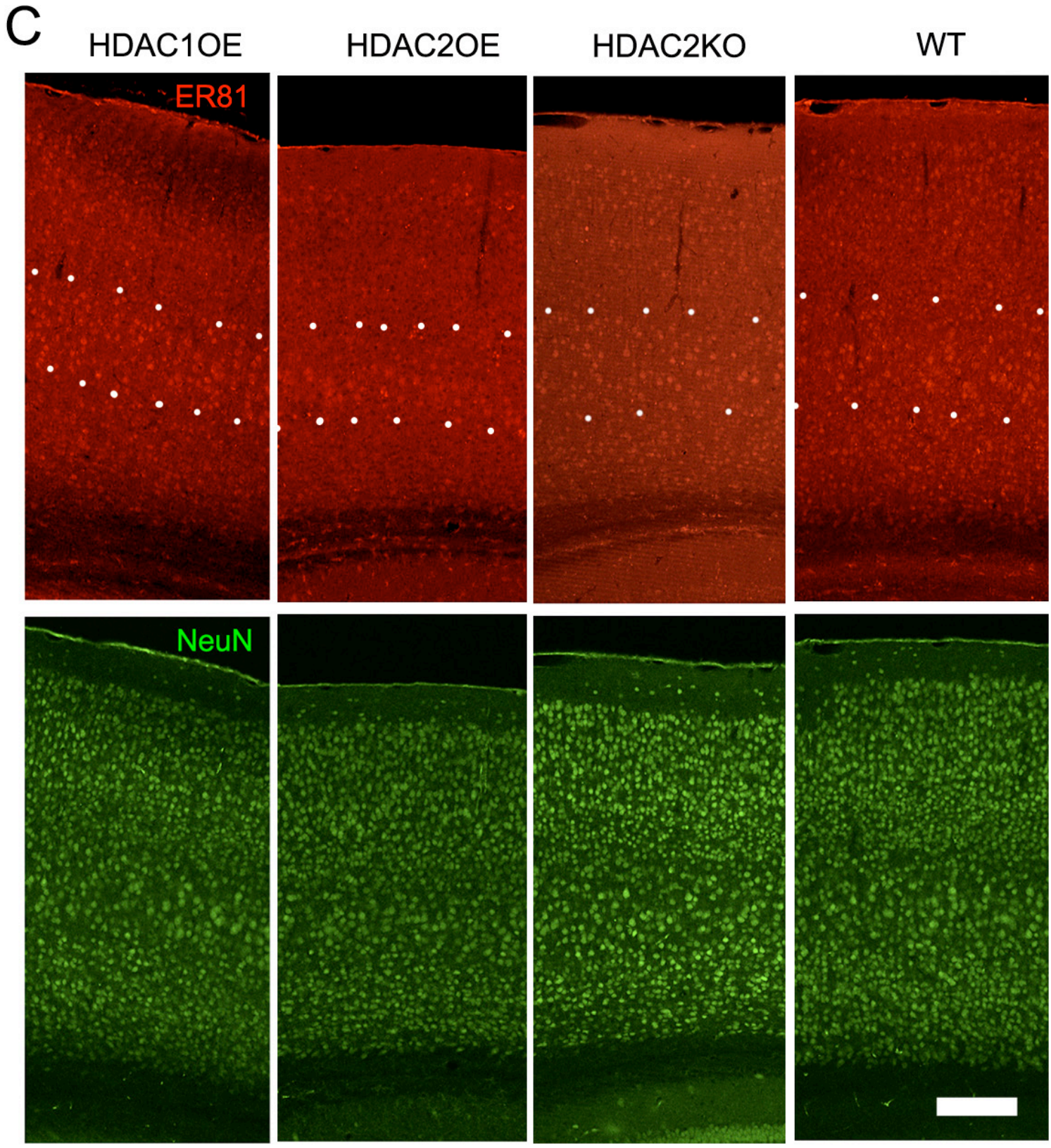
C
HDAC1OE
HDAC2OE
HDAC2KO
WT
ER81
NeuN

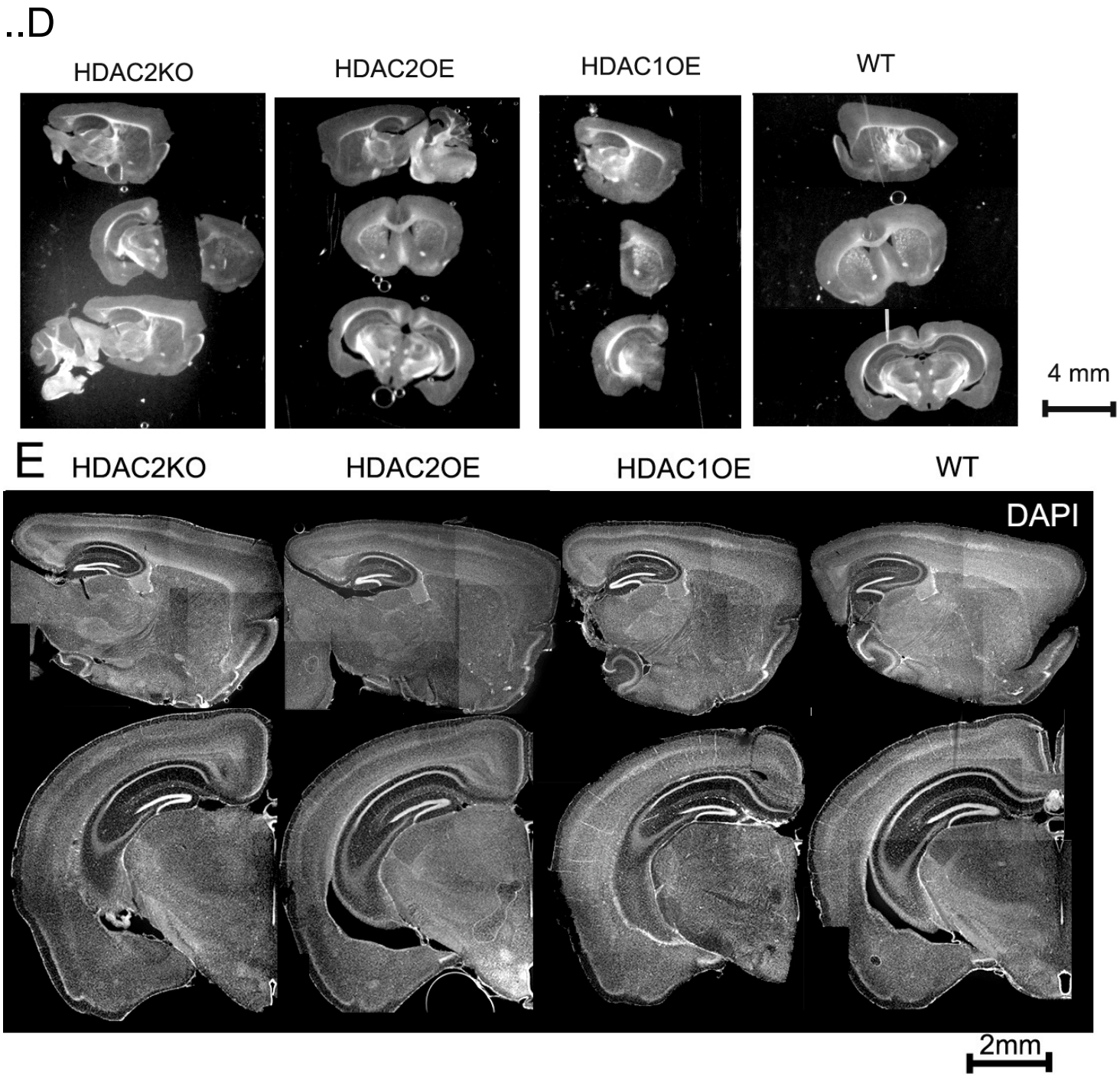

Supplemental Figure 12. Evaluation of brain morphology, neuronal fate and distribution of HDAC1OE, HDAC2OE and HDAC2KO mice.
(A-C). Cortical layering markers were used to examine the integrity of cortical lamination in HDAC1OE, HDAC2OE and HDAC2KO mice. Dashed lines show the distribution of immuno-positive neurons. Scale bar, 200 μm (A)Brn-1 labels layer II-V neurons. TLE4 labels deep layer neurons. No significant difference was found among HDAC1OE, HDAC2OE and HDAC2KO mice. (B) CDP(cux-1) labels layer II-IV neurons. No significant difference was detected among the 3 strains of mice. (C) ER-81 labels layer V and NeuN labels all neurons in the cortex. No obvious difference was detected among these mice. (D) Bright field images of coronal and sagittal sections of HDAC1OE, HDAC2OE and HDAC2KO mice. (E) DAPI staining of coronal and sagittal sections of HDAC1OE, HDAC2OE and HDAC2KO mice.

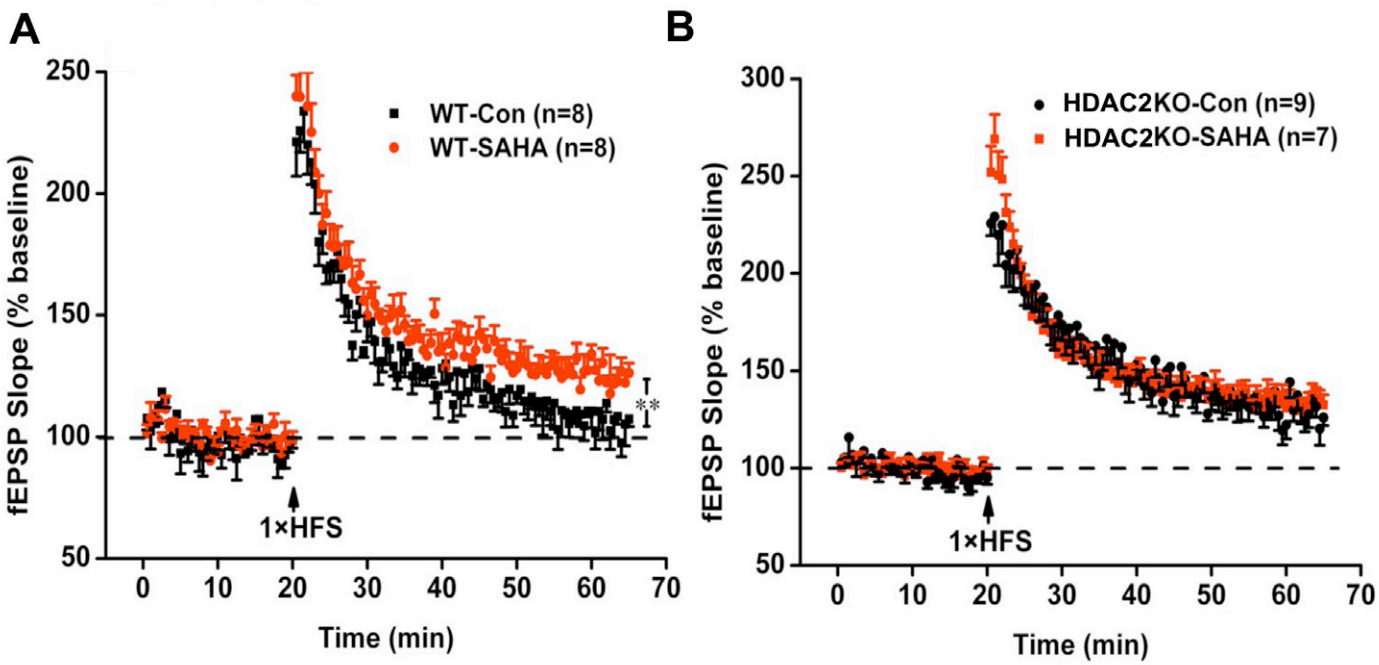

Supplemental Figure 13. SAHA treatment facilitates LTP in WT but not HDAC2KO hippocampus.
(A-B) One-month-old HDAC2KO mice and WT littermates were injected with SAHA (25 mg/kg, i.p.) or saline for 10 days. An additional injection was introduced 30 minutes before sacrifice. Long-term potentiation (LTP) was induced by one HFS stimulation (1 x 100Hz, 1s) of Schaffer collaterals. (A) A significant increase in the magnitude of LTP was observed in the SAHA treated WT mice when compared to the saline group. (B) No significant difference in the magnitude of LTP was detected between SAHA and saline-treated HDAC2KO mice (**, $p<0.005$, two-way ANOVA).

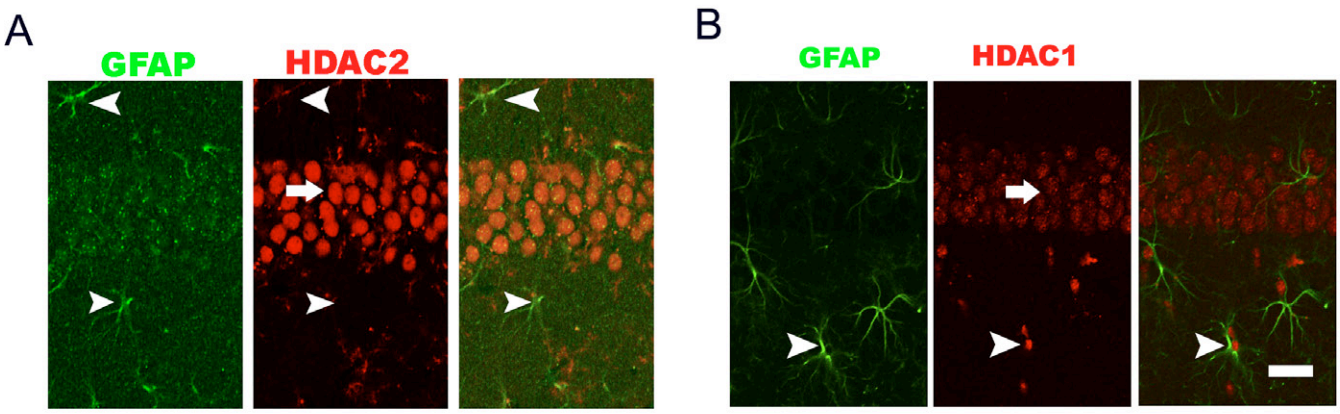

Supplemental Figure 14. Association of HDAC1 and HDAC2 with co-repressors.

(A-B) GFAP staining is in green and HDAC staining is in red. Arrows point to the pyramidal neurons in area CA1, arrowheads point to glial cells labeled by GFAP. Note that HDAC2 was primarily localized to the nucleus of pyramidal neurons, whereas HDAC1was detected in both neurons and glia. HDAC1 signal was higher in glia than in neurons. Scale bar, 100 μm.

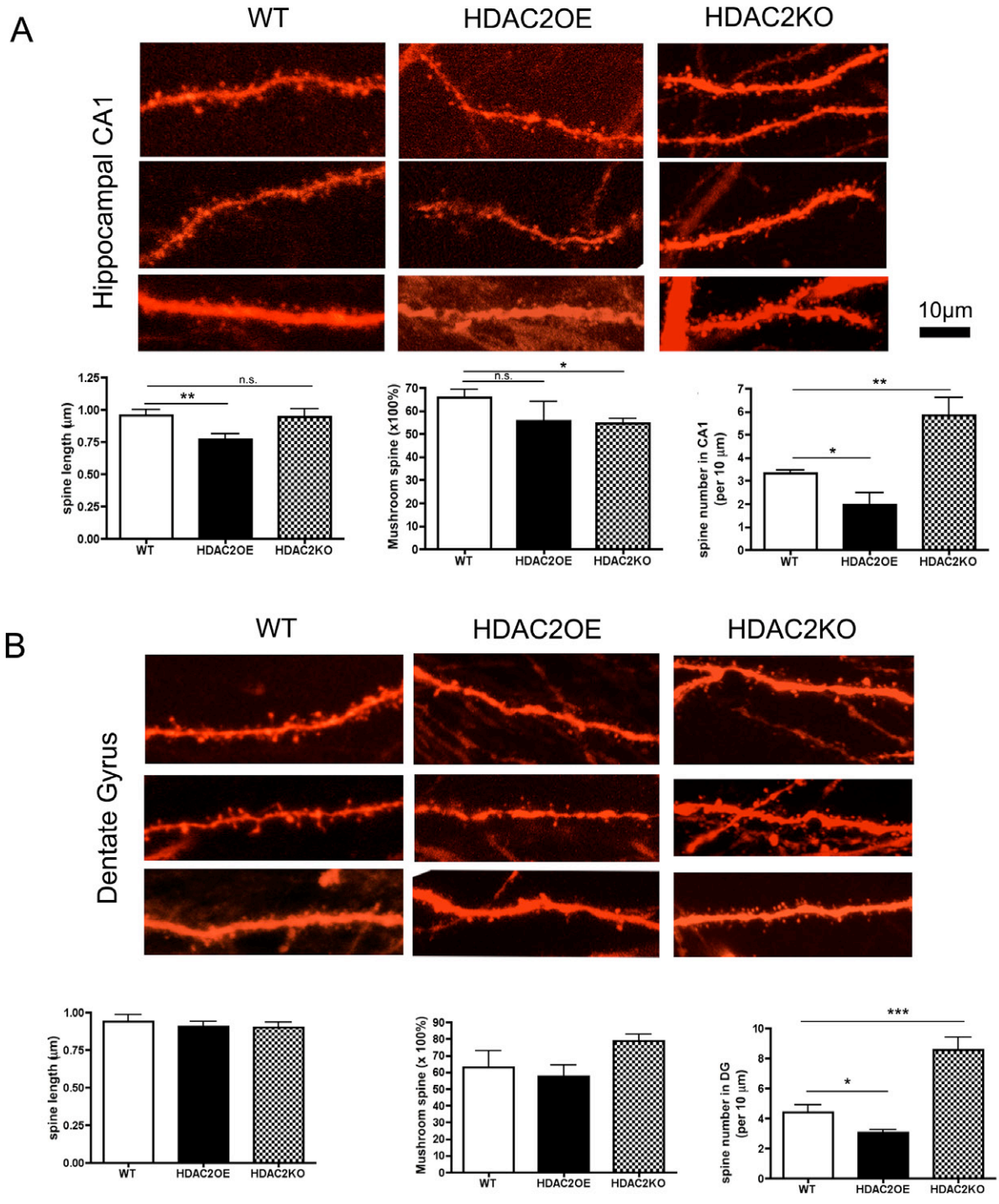

Supplemental figure 15. Characterization of dendritic spines in mouse models

(A-B) The length and density of dendritic spines, and the percentage of mushroom spines in HDAC2OE and HDAC2KO mice were measured in mouse brains by labeling neurons with tdTomoto using recombinant HSV. Changes in spine density could be detected in both area CA1 and dentate gyrus(DG). Spine length was reduced in area CA1 but not in DG of HDAC2OE mice. No change in spine length was detected in HDAC2KO mice. Percentage of mushroom spines decreased in area CA1 but not in DG. No significant change in the percentage of mushroom spine was detected in HDAC2OE mice in area CA1 and DG. Confocal stack images were 3D-reconstructed and all dendritic spines were analyzed using Image-J. For each genotype and each region, more than 12 segments of dendrites and all spines on the dendrites were analyzed and quantified (* $p<0.05$;**, $p<0.005$, ***, $p<0.001$, student *t*-test).

Thus, in area CA1, HDAC2OE mice exhibited a significant reduction in spine length, while no significant change was detected in HDAC2KO mice. Conversely, the percentage of mushroom spines was reduced in HDAC2KO mice, although no difference in mushroom spines was detected in HDAC2OE mice. Interestingly, in the DG, no significant changes in the spine length and proportion of mushroom spines were noted. As in the HDAC2OE and KO mice, changes in HDAC2 expression occur in all neurons; thus the discrepancies in the spine length and shape in different hippocampal areas suggest that HDAC2 may indirectly regulate spine morphology.

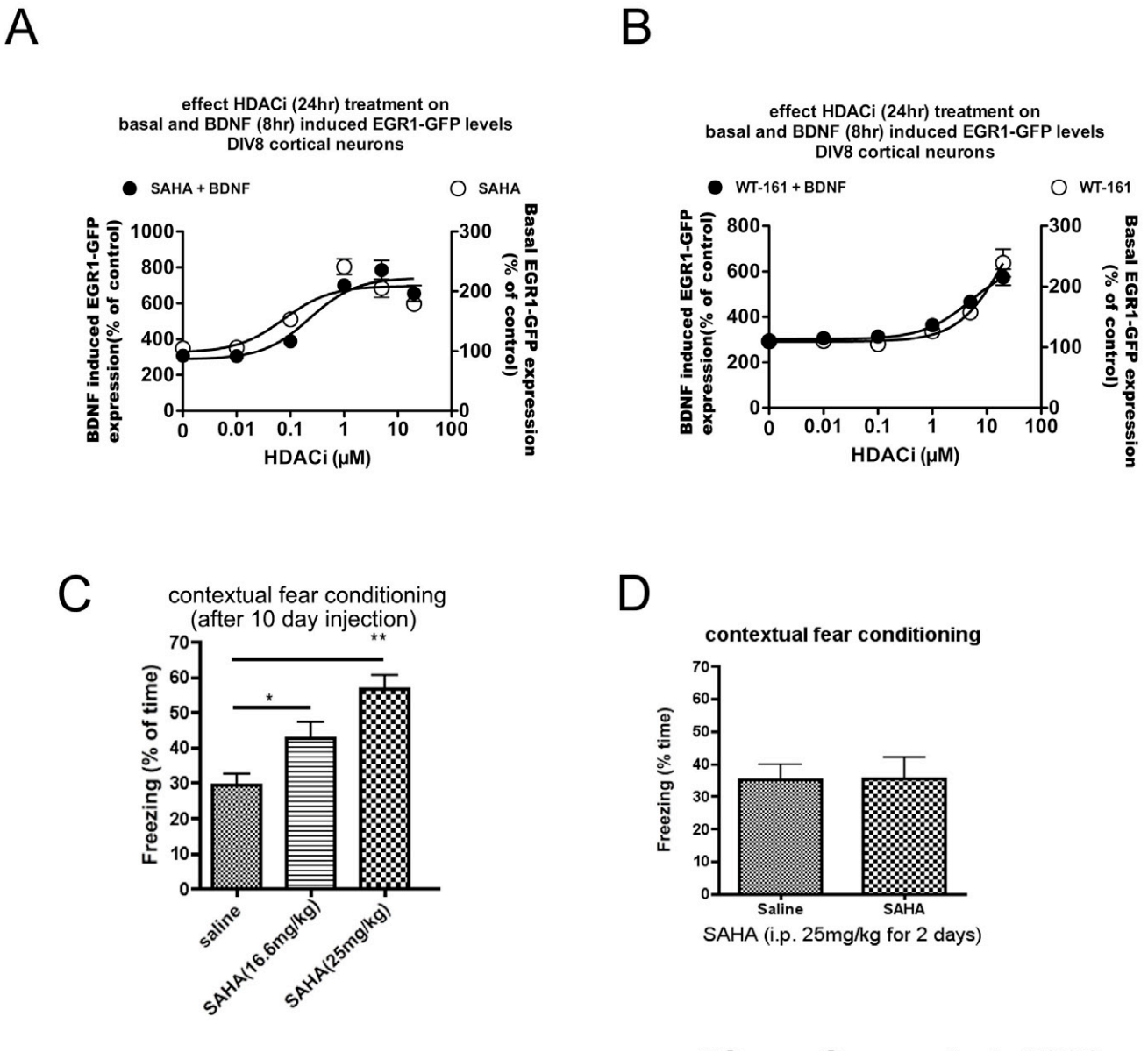

Supplemental figure 16. Dose response of HDAC inhibitors in cultured neurons and mice.

(A-B) Dose response curve of SAHA or WT-161 pre-treatment induced EGR1 expression in dissociated cortical neurons (treated with 40μM NBQX and 100μM AP5) with or without the induction of BDNF (50 ng/ml). With or without BDNF treatment, the EC_{50} of SAHA (~500 nM) is much lower than that of the EC_{50} WT-161 (>10 uM). (C) Memory test of WT mice injected with high dosage (25mg/kg) or low dosage (16.6 mg/kg) SAHA for 10 days. Mice were subjected to contextual fear conditioning training 24 hours before test (saline , n=20; SAHA (16.6mg/kg) (n=10, p=0.02, v.s. saline student *t*-test); SAHA (25 mg/kg), (n=10; p=0.001, student *t*-test). (D) Memory test of WT mice injected with SAHA (25mg/kg) for 2 days. Mice were subjected to contextual fear conditioning training 24 hours before test. (saline, n=10; SAHA, n=10) Saline group and SAHA group showed similar freezing levels in the memory test.

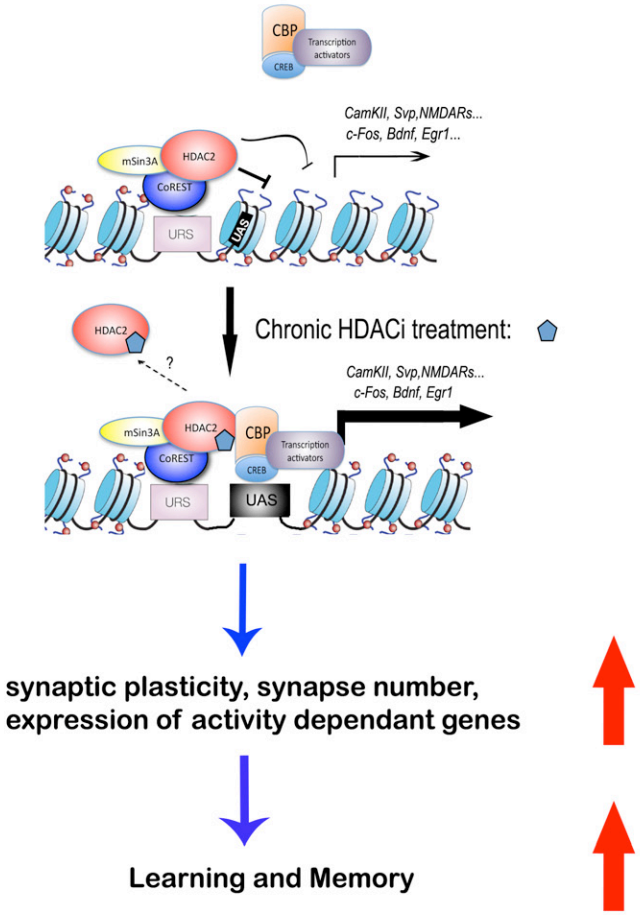

Supplemental figure 17. HDAC2 regulates learning and memory by suppressing neuronal gene expression

HDAC2 is present in the transcriptional repressor complexes containing CoREST and targets activity regulated genes. HDAC2 is the main target of HDAC inhibitors (HDACi) that facilitate memory formation by de-repressing HDAC2 target genes. HDACi treatment can lead to increased histone acetylation locally, resulting in relaxed chromatin structure and increased accessibility for transcription activation factors, such as CREB/CBP complexes. Transcriptional activation of CREB/CBP may further facilitate the expression of neuronal genes functioning in synaptic plasticity, learning and memory in part through its associated histone acetyltransferase activity..

5. Supplemental References

1 Goldberg, A. D., Allis, C. D., and Bernstein, E., Epigenetics: a landscape takes shape. *Cell* **128** (4), 635 (2007).

2 Yang, X. J. and Seto, E., The Rpd3/Hda1 family of lysine deacetylases: from bacteria and yeast to mice and men. *Nat Rev Mol Cell Biol* **9** (3), 206 (2008).

3 Sealy, L. and Chalkley, R., The effect of sodium butyrate on histone modification. *Cell* **14** (1), 115 (1978).

4 Tsankova, N. M. et al., Sustained hippocampal chromatin regulation in a mouse model of depression and antidepressant action. *Nat Neurosci* **9** (4), 519 (2006).

5 Renthal, W. et al., Histone deacetylase 5 epigenetically controls behavioral adaptations to chronic emotional stimuli. *Neuron* **56** (3), 517 (2007).

[6] Lahm, A. et al., Unraveling the hidden catalytic activity of vertebrate class IIa histone deacetylases. *Proc Natl Acad Sci U S A* **104** (44), 17335 (2007).
[7] Pandey, U. B. et al., HDAC6 rescues neurodegeneration and provides an essential link between autophagy and the UPS. *Nature* **447** (7146), 859 (2007); Hubbert, C. et al., HDAC6 is a microtubule-associated deacetylase. *Nature* **417** (6887), 455 (2002).
[8] McAllister, A. K., Lo, D. C., and Katz, L. C., Neurotrophins regulate dendritic growth in developing visual cortex. *Neuron* **15** (4), 791 (1995).
[9] Timmusk, T. et al., Multiple promoters direct tissue-specific expression of the rat BDNF gene. *Neuron* **10** (3), 475 (1993).
[10] Hrabetova, S. and Sacktor, T. C., Bidirectional regulation of protein kinase M zeta in the maintenance of long-term potentiation and long-term depression. *J Neurosci* **16** (17), 5324 (1996); Drier, E. A. et al., Memory enhancement and formation by atypical PKM activity in Drosophila melanogaster. *Nat Neurosci* **5** (4), 316 (2002); Shema, R., Sacktor, T. C., and Dudai, Y., Rapid erasure of long-term memory associations in the cortex by an inhibitor of PKM zeta. *Science* **317** (5840), 951 (2007).
[11] Jones, M. W. et al., A requirement for the immediate early gene Zif268 in the expression of late LTP and long-term memories. *Nat Neurosci* **4** (3), 289 (2001); Worley, P. F. et al., Constitutive expression of zif268 in neocortex is regulated by synaptic activity. *Proc Natl Acad Sci U S A* **88** (12), 5106 (1991).
[12] Bozon, B., Davis, S., and Laroche, S., Regulated transcription of the immediate-early gene Zif268: mechanisms and gene dosage-dependent function in synaptic plasticity and memory formation. *Hippocampus* **12** (5), 570 (2002).
[13] Bartsch, D. et al., Aplysia CREB2 represses long-term facilitation: relief of repression converts transient facilitation into long-term functional and structural change. *Cell* **83** (6), 979 (1995).
[14] Impey, S. et al., Stimulation of cAMP response element (CRE)-mediated transcription during contextual learning. *Nat Neurosci* **1** (7), 595 (1998).
[15] Pittenger, C. et al., Reversible inhibition of CREB/ATF transcription factors in region CA1 of the dorsal hippocampus disrupts hippocampus-dependent spatial memory. *Neuron* **34** (3), 447 (2002).
[16] Gass, P. et al., Deficits in memory tasks of mice with CREB mutations depend on gene dosage. *Learn Mem* **5** (4-5), 274 (1998).
[17] Guan, Z. et al., Integration of long-term-memory-related synaptic plasticity involves bidirectional regulation of gene expression and chromatin structure. *Cell* **111** (4), 483 (2002).
[18] Craig, A. M. and Kang, Y., Neurexin-neuroligin signaling in synapse development. *Curr Opin Neurobiol* **17** (1), 43 (2007); Chih, B., Engelman, H., and Scheiffele, P., Control of excitatory and inhibitory synapse formation by neuroligins. *Science* **307** (5713), 1324 (2005).
[19] Silva, A. J., Paylor, R., Wehner, J. M., and Tonegawa, S., Impaired spatial learning in alpha-calcium-calmodulin kinase II mutant mice. *Science* **257** (5067), 206 (1992); Silva, A. J., Stevens, C. F., Tonegawa, S., and Wang, Y., Deficient hippocampal long-term potentiation in alpha-calcium-calmodulin kinase II mutant mice. *Science* **257** (5067), 201 (1992).
[20] Cheung, Z. H., Fu, A. K., and Ip, N. Y., Synaptic roles of Cdk5: implications in higher cognitive functions and neurodegenerative diseases. *Neuron* **50** (1), 13 (2006); Fischer, A. et al., Cyclin-dependent kinase 5 is required for associative learning. *J Neurosci* **22** (9), 3700 (2002).
[21] Herdegen, T. et al., The KROX-20 transcription factor in the rat central and peripheral nervous systems: novel expression pattern of an immediate early gene-encoded protein. *Neuroscience* **57** (1), 41 (1993).
[22] van Zundert, B., Yoshii, A., and Constantine-Paton, M., Receptor compartmentalization and trafficking at glutamate synapses: a developmental proposal. *Trends Neurosci* **27** (7), 428 (2004); Migaud, M. et al., Enhanced long-term potentiation and impaired learning in mice with mutant postsynaptic density-95 protein. *Nature* **396** (6710), 433 (1998).
[23] Ksiazek, I. et al., Synapse loss in cortex of agrin-deficient mice after genetic rescue of perinatal death. *J Neurosci* **27** (27), 7183 (2007).

[24] Vazdarjanova, A. et al., Experience-dependent coincident expression of the effector immediate-early genes arc and Homer 1a in hippocampal and neocortical neuronal networks. *J Neurosci* **22** (23), 10067 (2002).
[25] Bottai, D. et al., Synaptic activity-induced conversion of intronic to exonic sequence in Homer 1 immediate early gene expression. *J Neurosci* **22** (1), 167 (2002); Jaubert, P. J. et al., Complex, multimodal behavioral profile of the Homer1 knockout mouse. *Genes Brain Behav* **6** (2), 141 (2007).
[26] Vazdarjanova, A. et al., Spatial exploration induces ARC, a plasticity-related immediate-early gene, only in calcium/calmodulin-dependent protein kinase II-positive principal excitatory and inhibitory neurons of the rat forebrain. *J Comp Neurol* **498** (3), 317 (2006); Chowdhury, S. et al., Arc/Arg3.1 interacts with the endocytic machinery to regulate AMPA receptor trafficking. *Neuron* **52** (3), 445 (2006).
[27] Greenberg, M. E., Hermanowski, A. L., and Ziff, E. B., Effect of protein synthesis inhibitors on growth factor activation of c-fos, c-myc, and actin gene transcription. *Mol Cell Biol* **6** (4), 1050 (1986).
[28] Fleischmann, A. et al., Impaired long-term memory and NR2A-type NMDA receptor-dependent synaptic plasticity in mice lacking c-Fos in the CNS. *J Neurosci* **23** (27), 9116 (2003).
[29] Matsuo, N., Reijmers, L., and Mayford, M., Spine-type-specific recruitment of newly synthesized AMPA receptors with learning. *Science* **319** (5866), 1104 (2008).
[30] Tarsa, L. and Goda, Y., Synaptophysin regulates activity-dependent synapse formation in cultured hippocampal neurons. *Proc Natl Acad Sci U S A* **99** (2), 1012 (2002).
[31] Samigullin, D., Bill, C. A., Coleman, W. L., and Bykhovskaia, M., Regulation of transmitter release by synapsin II in mouse motor terminals. *J Physiol* **561** (Pt 1), 149 (2004).
[32] Hung, A. Y. et al., Smaller dendritic spines, weaker synaptic transmission, but enhanced spatial learning in mice lacking Shank1. *J Neurosci* **28** (7), 1697 (2008); Ehlers, M. D., Molecular morphogens for dendritic spines. *Trends Neurosci* **25** (2), 64 (2002).
[33] Ohshima, T. et al., Impairment of hippocampal long-term depression and defective spatial learning and memory in p35 mice. *J Neurochem* **94** (4), 917 (2005).
[34] Cantallops, I., Haas, K., and Cline, H. T., Postsynaptic CPG15 promotes synaptic maturation and presynaptic axon arbor elaboration in vivo. *Nat Neurosci* **3** (10), 1004 (2000).
[35] Nedivi, E., Wu, G. Y., and Cline, H. T., Promotion of dendritic growth by CPG15, an activity-induced signaling molecule. *Science* **281** (5384), 1863 (1998).
[36] Liu, L. et al., Role of NMDA receptor subtypes in governing the direction of hippocampal synaptic plasticity. *Science* **304** (5673), 1021 (2004).
[37] Zhao, M. G. et al., Roles of NMDA NR2B subtype receptor in prefrontal long-term potentiation and contextual fear memory. *Neuron* **47** (6), 859 (2005).
[38] Sprengel, R. et al., Importance of the intracellular domain of NR2 subunits for NMDA receptor function in vivo. *Cell* **92** (2), 279 (1998).
[39] Chung, H. J., Steinberg, J. P., Huganir, R. L., and Linden, D. J., Requirement of AMPA receptor GluR2 phosphorylation for cerebellar long-term depression. *Science* **300** (5626), 1751 (2003).
[40] Pak, D. T. and Sheng, M., Targeted protein degradation and synapse remodeling by an inducible protein kinase. *Science* **302** (5649), 1368 (2003).